On the Contribution of Electric-Type Current Patterns to UISNR for a Spherical Geometry at 9.4 T

Andreas Pfrommer[1] and Anke Henning[1,2]

[1]*Max Planck Institute for Biological Cybernetics, Tuebingen, Germany,* [2]*Institute for Biomedical Engineering, UZH and ETH Zurich, Zurich, Switzerland*

Introduction: Theoretical considerations of the ultimate intrinsic signal-to-noise ratio (UISNR) in the past have shown that parallel imaging is limited by the Maxwell equations itself [1, 2]. A complete set of vector solutions to the Helmholtz wave equation consists on the one hand of curl-free (electric modes) and on the other hand of divergence-free fields (magnetic modes) [3, 4]. Both of them contribute to total UISNR. All closed surface loop array coils, however, are only able to excite the magnetic-type fields and therefore might miss important contributions from the electric modes to SNR at specific voxel positions. For example from previous investigations at 7T [5- 7], concerning a cylindrical phantom it is known that the curl-free component of the current contributes significantly to SNR at a central position. In this study we investigated the effect of the electric mode to total UISNR for different voxel positions and acceleration factors in a spherical geometry simplifying the human head.

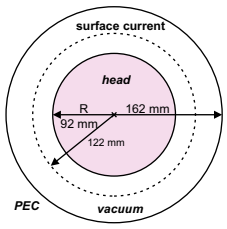

Figure 1: Three-layered spherical model for calculating UISNR by current mode expansion with DGF.

Methods: We solved the electromagnetic field problem in a spherically three-layered media model (s. fig. 1) by a current mode expansion with dyadic Green's functions (DGF) [8]. Thereby a surface current $\boldsymbol{K}$ was flowing on a sphere at a distance from the center (122 mm in our case). To excite both the magnetic- and electric type fields inside the head, the surface current density $\boldsymbol{K}$ had a divergence-free component $\boldsymbol{X}_{l,m}(\vartheta,\varphi)$ and a curl-free component $\hat{\boldsymbol{r}} \times \boldsymbol{X}_{l,m}(\vartheta,\varphi)$ (s. equation 1). The factors $c_{l,m}^{magn}$ and $c_{l,m}^{elec}$ were the expansion coefficients for the magnetic and electric mode respectively. In contrast to [2] we considered the influence of a spherical RF shield at a distance of 162 mm from the center of the global coordinate system and we assumed a perfect electric conductor (PEC). The innermost layer modelled the human head with a radius of 92 mm. We chose tissue equivalent values (averaged grey and white matter) for the permittivity and conductivity at 9.4T (ϵ_r= 49.8, conductivity = 0.59 S/m). Phase encoding and related acceleration by parallel imaging was chosen to be in x and y direction. All computations were done in custom written MATLAB (The Mathworks, Natick, USA) code. A Cartesian grid with spatial resolution of approx. 2.9 mm isotropically was used. The expansion order was carefully chosen to reach convergence of UISNR. By truncating the infinite series at an order of l=60 the relative change of UISNR at each voxel position was less than 1e-3 except for the peripheral voxel positions.

$$\boldsymbol{K}(\vartheta,\varphi) = \sum_l \sum_m c_{l,m}^{magn} \boldsymbol{X}_{l,m}(\vartheta,\varphi) + c_{l,m}^{elec} \left(\hat{\boldsymbol{r}} \times \boldsymbol{X}_{l,m}(\vartheta,\varphi) \right) \quad \text{(Equation 1)}$$

Results: In figure 2 we plotted the UISNR contribution of the magnetic modes to the total UISNR with contribution from both magnetic and electric modes in the planes z=0 and y=0. For that matter it is important to keep in mind that even for regions with the same relative contribution of electric and magnetic modes the resulting current patterns according to equation 1 depend on the specific voxel position and acceleration factors. Independently of the acceleration factor there was no UISNR gain by the electric mode in central voxel positions and at the periphery. For the non-accelerated case the maximum gain in UISNR by the electric mode was 55% at an intermediate voxel position. The mean gain in UISNR for all voxel positions was 24% (s. fig. 3). The UISNR gain did not change significantly with moderate acceleration up to 4x4 (mean 22%, max 53%). However going to very high 8x8 acceleration we recognized a saturation effect. The mean gain dropped down to 10% and even for intermediate voxel positions the electric modes could only improve UISNR by 19%. We believe that the reason for this saturation effect lies in the different power losses for magnetic and electric modes. In figure 4 the ratio of the electric mode power losses inside the head versus the magnetic mode power losses were plotted. The losses caused by the electric type current patterns increase much faster with the expansion order than the magnetic type losses do. In contrast to that for high acceleration factors especially the higher order terms of the series expansion become important to provide enough spatial variation in order to separate the aliased voxels. Therefore the magnetic modes are more favorable for higher degrees causing less power losses.

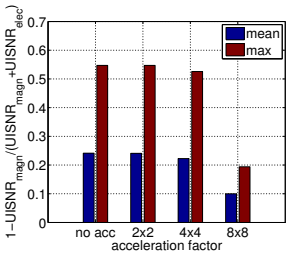

Figure 3: UISNR boost by the electric mode for different acceleration factors averaged on all voxel positions and maximum gain at intermediate voxel position.

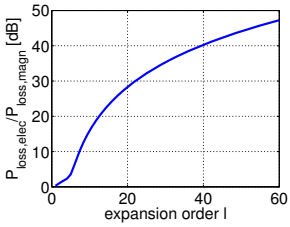

Figure 4: Ratio of power losses inside the "head" sphere for magnetic mode vs. electric mode current pattern.

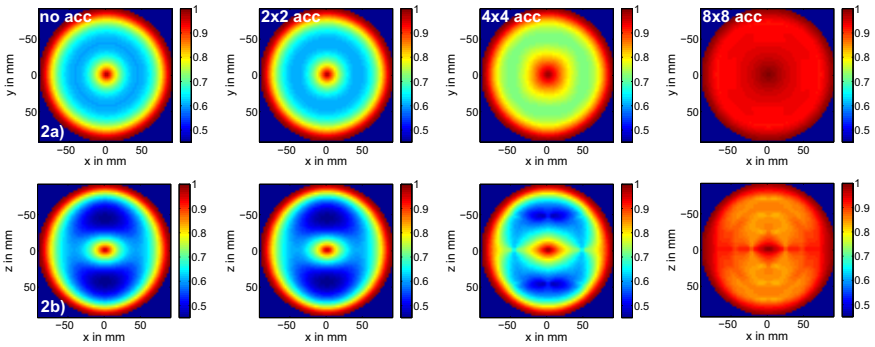

Figure 2: Contribution of the magnetic mode to UISNR as the ratio:

$$\frac{UISNR_{magn}}{UISNR_{magn}+UISNR_{elec}}$$

a) In the z=0 plane
b) In the y=0 plane

Conclusion: We have shown that for low to moderate acceleration electric modes can improve UISNR for large parts of the field of view inside a sphere with tissue equivalent properties at 9.4 T. For moderate two-dimensional k-space undersampling in x and y direction one can expect a mean UISNR improvement by slightly more than 20% and a maximum UISNR improvement by more than 50% at specific voxel positions due to the curl-free current pattern. For very high accelerations (e.g. 8x8) the UISNR is mostly contributed by the magnetic mode for all voxel positions.

References: [1] F. Wiesinger *MRM* 52, p. 376-390, 2004 [2] R. Lattanzi *MRM* 68, p. 286-304, 2012
[3] J. Jackson *Classical Electrodynamics* 3rd *ed.*, p. 429 ff. [4] C. Tai *Dyadic Green Functions in Electromagnetic Theory* 2nd ed., p. 198 ff.
[5] G. Wiggins, *Proc. 20th ISMRM 2012*, p. 541 [6] G. Wiggins, *Proc. 21st ISMRM 2013*, p. 2737
[7] G. Chen, *Proc. 22nd ISMRM 2014*, 402 [8] L. Li, *IEEE Trans. Microwave Theory* 42, p. 2302-2310, 1994